Targeting oncogenic transcription in prostate cancer with a novel, oral bioavailable, and ultra-selective CDK9 inhibitor

André Richters,1,2,3 Shelby K. Doyle,1,2,3,4, David Freeman5, Christina Lee5, Florian Kabinger1, Becky S. Leifer1-3, Sajjeev Jagannathan6, Jošt Vrabič Koren6, Deep Chatterjee7, Sebastian Mathea7, Julie Urgiles1, Nicholas B. Struntz1-3, Ryan A. Stagg8, Brice H. Curtin1-3, Joshua W. Russo9, Peter J. Mikochik5, Tamara D. Hopkins5, Hua Gao5, Kristen L. Karlin6, Calla M. Olson6, Joseph Vacca5, Chris Wilfong5, Wes Trotter5, Doug Saffran5, Norbert Bischofberger5, Stefan Knapp7, Steven P. Balk9, Ian Hickson10, Charles Y. Lin5,6,11, Marius S. Pop5, Angela N. Koehler1-4

Abstract

Castration resistant prostate cancers (CRPCs) lose sensitivity to androgen deprivation therapies but frequently remain dependent on oncogenic transcription driven by androgen receptor (AR) and its splice variants. To discover novel modulators of AR isoform activity, we identified binders of AR variants and their interactome members using a lysate-based small molecule microarray (SMM) screening assay and identified KI-ARv-03 as a putative binder that reduces AR levels and proliferation in prostate cancer cells. We deduce KI-ARv-03 to be a potent, selective inhibitor of CDK9, an important cofactor for AR, MYC, and other oncogenic transcription factors. Further optimization resulted in KB-130742, an orally bioavailable, selective CDK9 inhibitor with potent anti-tumor activity in CRPC models. In 22Rv1 cells, KB-00130742 rapidly downregulates nascent transcription, preferentially depleting short half-life transcripts and AR-driven oncogenic programs. In vivo, oral administration of KB-00130742 significantly reduced tumor growth in CRPC, supporting CDK9 inhibition as a promising therapeutic strategy to target AR dependence in CRPC.

I. ARv SMM screen funnel

A) SMM screen to identify binders of ARv complex

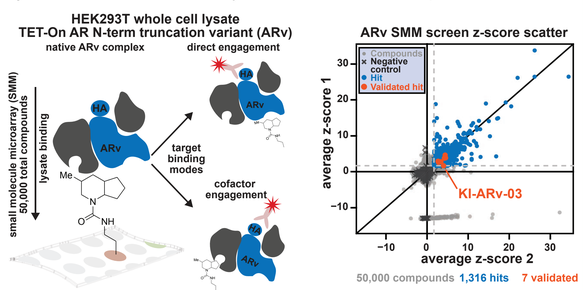

A) Left: SMM assay principle. Small molecule compounds are immobilized on a glass surface and a subset is capable of binding the desired target either directly or indirectly via an essential interaction partner. **Right:** Scatter plot of high-throughput SMM screening data of 50,000 compounds against an N-terminal HA-tagged AR-ΔLBD truncate. Initial assay positives (blue) and validated compounds (orange) including KI-ARv-03 cluster in the upper right panel.

B) Screen funnel to identify modulators of ARv dependency

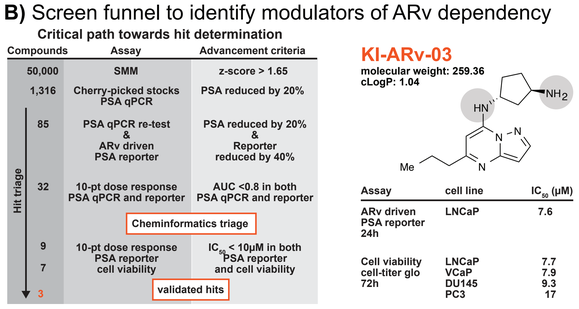

B) Left: Critical path to hit determination leads to three validated probe candidates after multiple rounds of secondary screening involving qPCR for PSA levels, AR driven PSA reporter gene assays, and cell viability. Validated hits exhibited dose-dependent downregulation of PSA, PS-driven reporters, and dose-dependent viablity effects on AR-dependent prostate cancer cell lines. **Right:** Chemical structure of KI-ARv-03 which was triaged as a lead probe candidate based on favorable performance in reporter and cell viability assays, physicochemical properties, and synthetic accessibility. KI-ARv-03 Reporter and cellular viability IC50s are shown. Intrinsic nucleophiles for SMM surface immobilization are highlighted in grey.

II. KI-ARv-03 is a selective CDK9 inhibitor

A) KI-ARv-03 pan-kinase profiling

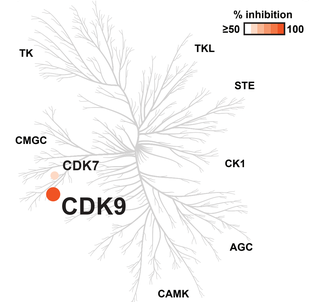

B) KI-ARv-03 CDK inhibition assay

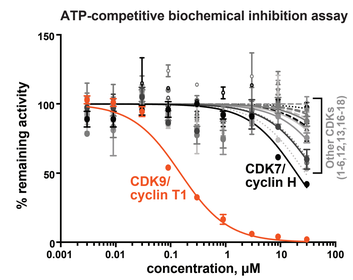

C) KI-ARv-03 interacts with CDK9 in cells

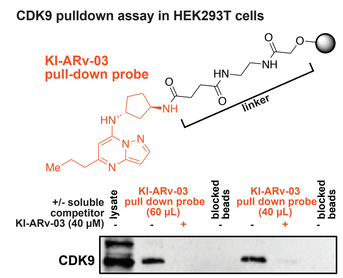

A) Phylogenetic tree representation of molecular kinase targets of KI-ARv-03 profiled against a panel of 413 kinases using the Eurofins KinaseProfilerTM technology. Circles indicate kinases with less than 50% remaining activity upon treatment with 10µM KI-ARv-03. CDK9 emerges as the dominant kinase target with near 100% biochemical inhibition at 10µM **B)** Dose-response curves for biochemical inhibition of a focused CDK panel after KI-ARv-03 treatment (n = 2 technical replicates, error bars represent mean ± SD). **C)** KI-ARv-03 (orange) covalently bound to solid support (black, Affi-Gel 10 beads) via the compound's terminal primary amine using N-hydroxysuccinimide (NHS) facilitated amide formation. **D)** Target engagement studies using KI-ARv-03 displayed on agarose beads (Affi-Gel 10) and 22Rv1 cell lysates. Control beads are terminally functionalized with ethanolamine and show no engagement of CDK9 or AR. KI-ARv-03 beads display reversible engagement of the most abundant isoform of CDK9 (42 kD).

III. KB-00130742 lead has increased potency and maintains selectivity

A) Model of KI-ARv-03 CDK9 recognition

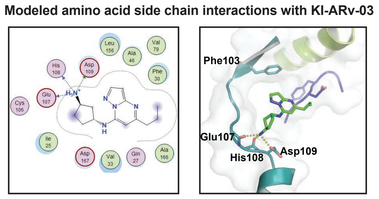

B) CDK9 inhibition of KI-ARv-03 and KB-0013742

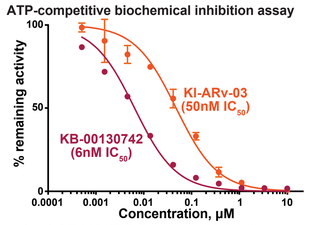

C) Fold selectivity of KI-ARv-03 and KB-0013742 on CDK9 vs. other CDKs

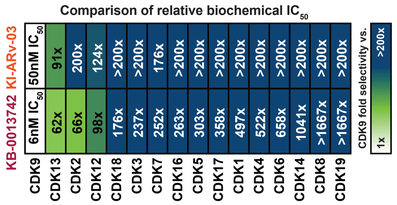

A) Molecular docking of KI-ARv-03 into the ATP binding cleft of CDK9 (PDB-code: 3MY1) suggesting ATP-competitive inhibition mode (type I). Color code: Hinge (teal), DFG-motif (blue), Helix αC (lime). Yellow spheres indicate hydrogen bonds. **B)** Dose-response curves for biochemical CDK9/Cyclin T1 inhibition after treatment with KI-ARv-03 and KB-00130742 (n = 2 technical replicates, error bars represent mean ± SD). **C)** Heatmap representation of biochemical inhibition of CDK family members by KI-ARv-03 and KB-00130742. Optimization of KI-ARv-03 results in KB-00130742, a single digit nM potent CDK9 inhibitor with greater than 60x fold selectivity vs. other CDKs

IV. Selective CDK9 inhibition blocks oncogenic nascent transcription

A) CDK9 inhibition globally downregulates nascent transcription

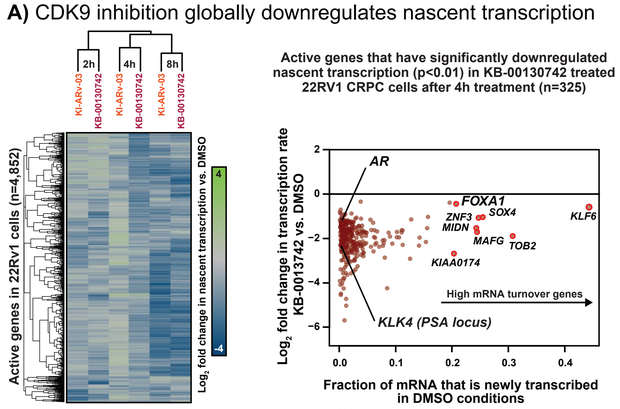

A) Left: Heatmap of active genes in 22Rv1 cells showing changes in nascent transcription level upon treatment over time. Gene rows are hierarchical clustered. By 8 hours, CDK9 inhibition results in global loss of nascent transcription. **Right:** Scatter plot of genes significantly downregulated (p<0.01) after 4h KB-00130742 treatment. Y-axis shows the log2 fold change in nascent transcription. Biologically relevant genes in CRPC are highlighted (*AR, KLK4*) as well as genes with high mRNA turnover that are significantly downregulated (e.g. *FOXA1, SOX4*).

B) CDK9 inhibition downregulates AR-dependent oncogenic transcription

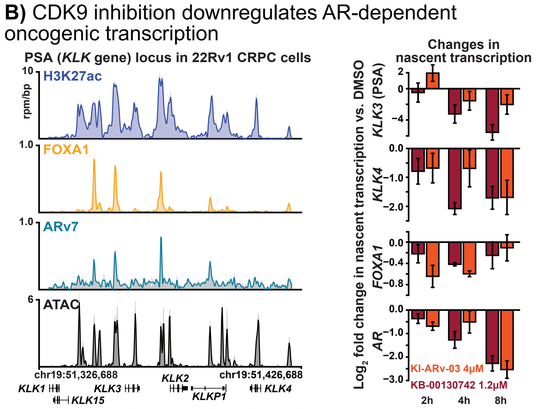

B) Left: Gene tracks of the PSA (*KLK*) locus showing chromatin acetylation (H3K27ac), transcription factor occupancy (FOXA1 and AR), and chromatin accessibility (ATAC). **Right:** Bar plots showing change in nascent transcription levels for key CRPC genes over time. Error bars represent standard error of the mean. High turnover genes such as *FOXA1* show earlier downregulation, while genes such as *KLK3* (PSA) and AR are downregulated at later timepoints, consistent with global effects of CDK9 inhibition.

V. *In vitro* activity of CDK9 inhibition

A) Selective CDK9 inhibition reduces tumor cell growth

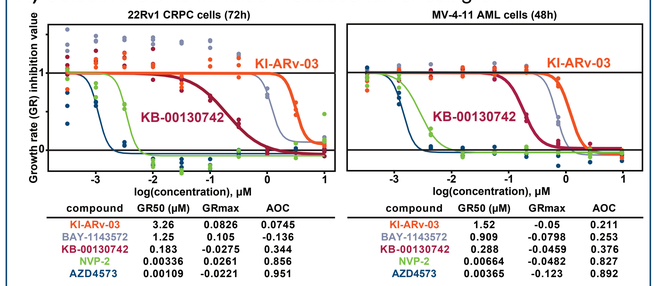

compound	GR50 (µM)	GRmax	AOC
KI-ARv-03	3.26	0.0826	0.0745
BAY-1143572	1.25	0.105	-0.136
KB-00130742	0.183	-0.0275	0.344
NVP-2	0.00336	0.0261	0.856
AZD4573	0.00109	-0.0221	0.951

compound	GR50 (µM)	GRmax	AOC
KI-ARv-03	1.52	-0.05	0.211
BAY-1143572	0.909	-0.0798	0.253
KB-00130742	0.288	-0.0459	0.376
NVP-2	0.00664	-0.0482	0.827
AZD4573	0.00365	-0.123	0.892

B) Selective CDK9 inhibition induces apoptosis

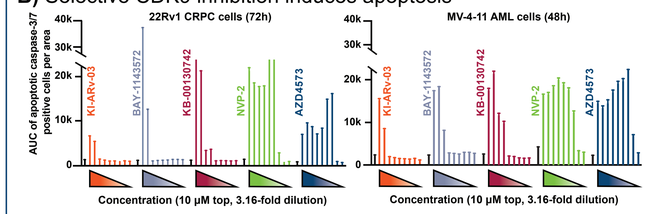

C) Selective CDK9 inhibition downregulates elongating RNA Pol II leading to loss of AR and MYC protein

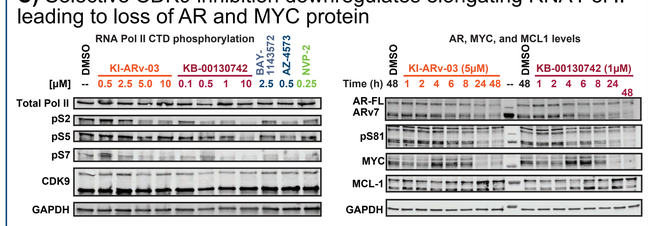

A) Dose-response curves and growth rate inhibition (GR) of 22Rv1 CRCP cells and MV-4-11 AML cells (treatments at 0-40µM, n = 3 technical replicates). **B)** Induction of apoptosis in 22Rv1 and MV-4-11 cells monitored as function of caspase 3/7 activation (treatments at 0-10 µM, n = 3 technical replicates). **C) Left:** Dose-response immunoblot of CDK9 and (phospho)-RNA Pol II levels in 22Rv1 after 6h treatment. **Right:** Time course immunoblot of AR, ARv7, AR phosphorylation, MYC, and MCL-1 protein levels in 22Rv1.

VI. *In vivo* activity of CDK9 inhibition

A) Selective CDK9 inhibition reduces tumor growth *in vivo*

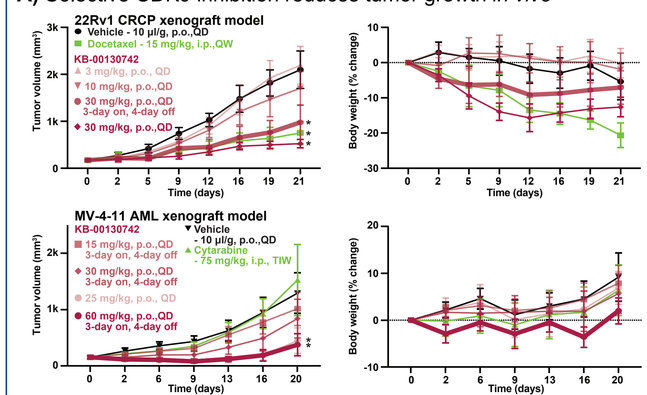

A) Left: tumor growth inhibition curves and **right:** precent body weight curves of different treatment groups (n = 10) in cell line xenografts of **top:** male CB17-SCID mice bearing 22Rv1 CRPC cells and **bottom:** female BALB/c nude mice bearing MV-4-11 AML cells. Data points represent group mean body weight. Error bars represent mean ± SEM. * represent significant (p<0.05) effect vs. vehicle. Intermittent (3-day on/4-day off) KB-00130742 treatment (bolded lines) significantly inhibits tumor growth with modest effects on body weight.